Supporting Information (SI)

for

Scalable Synthesis of Collagenic-Waste and Natural Rubber-Based Biocomposite for Removals of Hg(II) and Dyes: Approach for Cost-Friendly Waste Management

Nayan Ranjan Singha,*[,a] Chandan Roy,[a,b] Manas Mahapatra,[a] Arnab Dutta,[a] Joy Sankar Deb Roy,[a] Madhushree Mitra,[b] and Pijush Kanti Chattopadhyay*[,b]

[a]Advanced Polymer Laboratory, Department of Polymer Science and Technology and [b]Department of Leather Technology, Government College of Engineering and Leather Technology (Post Graduate), Maulana Abul Kalam Azad University of Technology, Salt Lake, Kolkata-700106, West Bengal, India.

Corresponding Author

*E-mail: drs.nrs@gmail.com (N.R.S.)

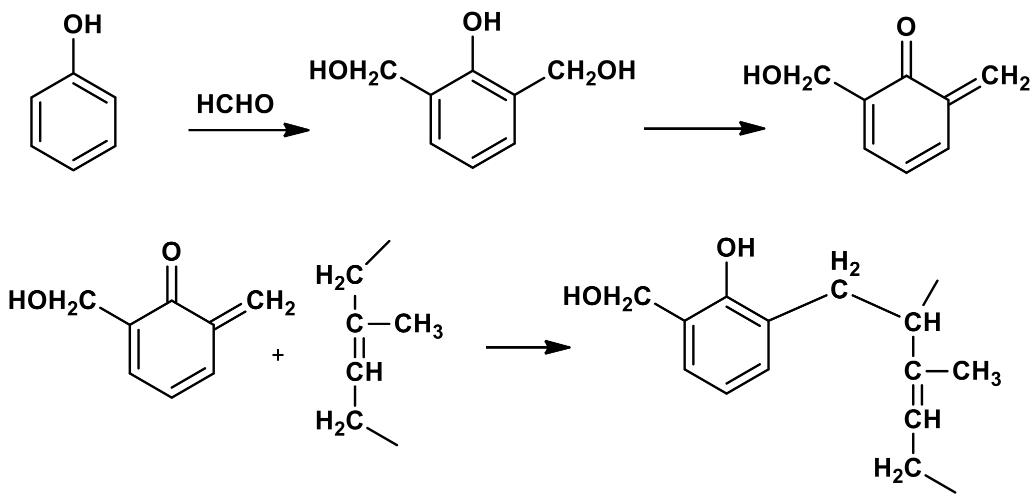

Scheme S1. Allyl hydrogen mechanism proposed by van der Meer

Table S1 Relative intensities of NR and NRCBD

	NR					remarks
assignment	**C_α**	**C_β**	**C_γ**	**C_δ**	**C_ε**	
δ (ppm)	135.16	124.99	32.17	26.36	23.37	pure NR, devoid of pendent double bond and having the equal proportion of each fragment
relative intensity	0.17	0.20	0.23	0.22	0.17	
	NRCBD					
δ (ppm)	135.13	125.75	32.68	26.78	23.94	significantly reduced intensity in C_α and C_β of NR in NRCBD confirmed reaction between >C=C< of NR and phenolic component of CBD during high temperature curing.
relative intensity	0.05	0.06	0.20	0.27	0.41	

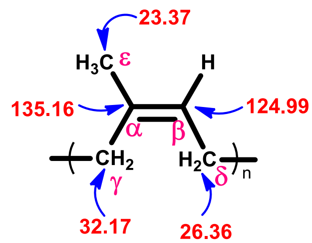

Table S2. FTIR analyses for NR, CBD, NRCBD, SF-, BCB-, and Hg(II)-NRCBD

FTIR peaks (cm^{-1})						significance(s)
NR	**CBD**	**NRCBD**	**SF-NRCBD**	**BCB-NRCBD**	**Hg(II)-NRCBD**	
–	–	–	–	–	3910, 3789	O–H *str.*
–	–	–	–	–	3846	O–H *str.* of HHg (OH) deposits
–	–	–	–	–	3827 (w)	O–H *str.* of $Hg(OH)_2$ deposits formed at pH > 5.0 during adsorption
–	3405 (b, vs)	3399 (b, s)	3399 (b, m)	3429 (b, m)	3433, 3409, 3399 (b, m)	N–H/O–H mutual H-bonding, new peaks at 3409 and 3433 in Hg(II)-NRCBD was due to binding of Hg(II) with N–H
3283 (b, w)						N–H/C–H mutual H-bonding (protein impurities in NR)[S1]
–	3088 (sh)	3088 (sh)	3078 (sh)	3066 (sh, vw)	3083 (vw)	aromatic ring C–H
3036	–	3040 (w)	3043 (sh, vw)	3041 (w)	3042 (vw)	C=C–H of NR[30]
2959 (w)	2957(vw)	2962(w)	2962 (w)	2962 (w)	2961 (sh)	*asym. str.* $–CH_3$[30]
2928	2927	2927	2928	2923	2927	*sym. str.* $–CH_3$[30]
2915	–	–	–	–	–	*sym. str.* of $–CH_3$ / $>CH_2$ adjacent to C=C splits into two in NR (i.e., 2928 and 2912)
2851	2854	2854	2855	2853	2856	*sym. str.* of $–CH_2$
2725	-	2727	2728	2727	–	*def. asym.* $–CH_3$ overtone[30]
–	2117 (br, w)	2107 (br, w)	2120 (br, w)	2096 (br, vw)	–	$>NH^+–$, $>C=NH^+–$ and $>NH_2^+$; vanished in Hg(II)-NRCBD due to Hg/N interaction
1748–1738	–	–	–	–	–	ν R1–(C=O)–O–R2 (Lipids)[30]
1711	–	–	–	–	–	ν R1–(C=O)–OH (Lipids)[30]
1663, 1657, 1630	1660, 1649, 1635	1660, 1647, 1635	1661, 1646	1660 (vw), 1647	1659 (vw), 1646	secondary amide I / C=C str.
1541	1548	1546	1551	1545	1546	*asym.* $–COO^-$/Amide II : βN–H + ν C–N)[30]
1446	1452	1450	1451	1449	1451	$–CH_2–$ scissoring[35]
–	1408	1406 (sh)	1406 (vw)	1402 (w)	–	*sym.* $–COO^-$
1377, 1361	1385 (vw)	1376	1377	1376	1382, 1378	*asym.* $–CH_3$
–	1334	1332	1334	1333 (vw)	–	amide-III; vanished in Hg(II)-NRCBD due to binding of Hg(II) with N–H
–	1318 (sh)	1317	1318 (vw)	1316 (vw)	1318 (b, vw)	ν C(4)–C(5) + ν C(3)–C(4) + ν C(1)–C(6) of chromane[31]
1310	–	–	–	–	–	δ *asym.* $–CH_3$[30]
1288	–	–	–	–	–	β C=C–H of NR; consumption of C=C of NR in NR-CBDs *via* chromane formation[30]
1246	1239	1239 (b,w)	1240	1238	1240	ν C(9)–O(2) + ρ $C(10)H_2$ of chromane[31]/sulfonic acid salts
–	1201	1195 (w)	1201	1196	1197	sulfonic acid salts
–	1158	1156 (b,w)	1161	1155 (b, vw)	1156	δ C(3)–H + δ C(2)–H of chromane[31]/ glycoside
1128	1119	1126	1124 (vw)	1124	1124	ρ $C(13)H_3$ + τω $C(10)H_2$ of chromane[31]/ ν C–C + ω–CH_2 of NR[30]
1090	–	1097	1096	1098	1100 (vw)	τ–CH_2 of NR[30]
1009	–	–	–	–	–	ν C–C[30]
984	–	–	–	–	–	τ C=C peak of NR; consumption of C=C of NR in NR-CBDs *via* chromane formation[30]
930	922 (vw)	926 (vw)	–	–	–	ν C–C[30]
840	–	837(vs)	837	838	840 (sh)	γ C=C–H (cis-1,4 addition) of NR[30]
–	805	–	–	–	–	triazine ring of melamine
–	780	780	780	–	781 (vw)	oxolated Cr-complex
741	–	–	–	–	–	ρ $–CH_2–$[30]
–	670	659	659 (vvw)	657 (vw)	658	sulfonic acid salts
–	603	600	–	–	600	δ C=O + δ C(3)–H of chromane[31]/sulfones
567	-	572 (b)	563	573	–	δ C(5)C(11)C(10) + δ C(1)C(6)C(5) + δ C(2)C(3)C(4) of chromane[31]
490	–	–	–	–	–	β C–C–C[30]

b = broad; ν: stretching, δ: in-plane deformation, γ: out-of-plane deformation, ρ: rocking, ω: wagging, τω: twisting, τ: torsion modes

Table S3. XPS analyses for NRCBD, Hg(II)-, BCB-, and SF-NRCBD

orbital	NRCBD	Hg(II)-NRCBD	BCB-NRCBD	SF-NRCBD	assignment
C1s	284.87	284.97	284.89	284.90	–**C**H_2–/–**C**H_3 of chromane, phenol
	285.33	285.50	285.42	285.58	tertiary **C**–H
	285.75	285.91	285.91	286.13	**C**1 of phenol
	286.15	286.26	286.34	286.74	$\mathbf{C}_{\alpha}$ of amino acid
	286.50	286.71	286.75	287.18	**C**2 of chromane ring and ether
	286.87	287.15	287.04	287.39	>**C**=N of melamine/ –**C**ONH_2/–**C**ONH–/–**C**OOH
O1s	530.20	531.18	530.81	530.60	polysaccharides or GAGs
	531.02	531.61	531.76	531.49	Cr(**O**H)$_3$
	532.06	532.25	532.00	532.29	>C=**O**
	532.82	532.83	532.62	532.94	chromane/ether/–CO**O**$^-$
	533.67	533.78	533.67	533.72	**O**–H
N1s	398.05	398.83	–	–	pyrrolidine units of proline/ hydroxyproline; coordinate bonding with Hg(II) in Hg(II)-NRCBD
	399.67	403.95	–	–	–**N**H–/–**N**H_2/C–**N** of collagen; coordinate bonding with Hg(II)
Hg 4f$_{7/2}$ (102.58 eV) and **4f$_{5/2}$** (106.68 eV)		100.93			coordinate bonding
		104.63			coordinate bonding

Table S3 (Continued)

	polysaccharides/GAGs /ZnO	$Cr(OH)_3$/ $Zn(OH)_2$	>C=O	chromane/ether/ –COO^-	O–H
O1s of NRCBD (eV)	530.20	531.02	532.06	532.82	533.67
relative intensities (%)	0.01	0.26	0.29	0.21	0.22
O1s of Hg-NRCBD (eV)	531.18	531.61	532.25	532.83	533.78
relative intensities	0.14	0.07	0.14	0.34	0.30[@]
O1s of BCB-NRCBD (eV)	530.81	531.76	532.00	532.62	533.67
relative intensities	0.11[#]	0.42[#]	0.02	0.34	0.10
O1s of SF-NRCBD (eV)	530.60	531.49	532.29	532.94	533.72
relative intensities	0.04	0.23	0.31	0.25	0.17

[@] deposited $Hg(OH)_2$ on Hg-NRCBD
[#] deposited ZnO and $Zn(OH)_2$ on BCB-NRCBD

Table S3 (Continued)

	CH_2/ CH_3 of chromane, phenol	tertiary CH	phenol	C_α	C2 of chromane ring, ether	>C=N of melamine/ $CONH_2$/ CONH–/ COOH
C1s of NRCBD (eV)	284.87	285.33	285.75	286.15	286.50	286.87
relative intensities	0.023	0.28	0.245	0.108	0.205	0.139
C1s of Hg-NRCBD (eV)	284.97	285.5	285.91	286.26	286.71	287.15
relative intensities	0.083	0.195	0.154	0.158	0.121	0.288
C1s of BCB-NRCBD (eV)	284.89	285.42	285.91	286.34	286.75	287.04
relative intensities	0.039	0.156	0.286	0.327	0.171	0.021
C1s of SF-NRCBD (eV)	284.9	285.58	286.13	286.73	287.18	287.39
relative intensities	0.097	0.115	0.164	0.204	0.255	0.165

Table S4 Design of experiment of CCD for SF/BCB

run no.	concentration of dyes (mg L^{-1}, A)	temperature (°C, B)	pH_i for SF/BCB (–, C)	actual ACs of SF/BCB (mg^{-1} g)	predicted ACs of SF/BCB (mg^{-1} g)
1	10.00	30.00	8.00/7.00	05.02/06.42	03.55/05.02
2	40.00	30.00	8.00/7.00	44.21/30.21	45.04/28.69
3	10.00	50.00	8.00/7.00	20.76/14.76	20.35/14.59
4	40.00	50.00	8.00/7.00	56.76/34.76	58.03/33.14
5	10.00	30.00	12.00/11.00	13.53/19.53	12.69/20.91
6	40.00	30.00	12.00/11.00	42.40/30.40	43.25/30.33
7	10.00	50.00	12.00/11.00	24.54/17.54	24.14/18.82
8	40.00	50.00	12.00/11.00	48.98/21.98	50.88/23.14
9	1.00	40.00	10.00/9.00	02.47/02.47	04.69/01.64
10	50.24	40.00	10.00/9.00	60.75/18.75	58.13/19.84
11	25.00	23.18	10.00/9.00	36.18/30.18	36.76/31.02
12	25.00	56.82	10.00/9.00	58.51/33.51	57.31/33.01
13	25.00	40.00	6.64/5.64	23.48/26.48	23.52/29.17
14	25.00	40.00	13.00/12.36	32.46/36.46	31.64/34.11
15	25.00	40.00	10.00/9.00	56.25/58.20	56.26/58.20
16	25.00	40.00	10.00/9.00	56.25/58.20	56.26/58.20
17	25.00	40.00	10.00/9.00	56.25/58.20	56.26/58.20
18	25.00	40.00	10.00/9.00	56.25/58.20	56.26/58.20
19	25.00	40.00	10.00/9.00	56.25/58.20	56.26/58.20
20	25.00	40.00	10.00/9.00	56.25/58.20	56.26/58.20

Table S5. Comparison table

name of adsorbate	name of adsorbent	adsorption capacities (mg g^{-1}) /pH/C_0 (mg L^{-1})/temperature (K)	ref.
BCB[a]	dimethyl terephthalate distillation residue	13.00/–/500/298	S2
	natural clay	42.00/–/50–500/–	S3
	CPCMC[a]	82.22/6.9/10–140/303	S4
	SPACMC[b]	83.73/6.3/10–140/303	S4
	PAACMC[c]	86.85/6.9/10–140/303	S4
	sulfonated Phenol-Formaldehyde resin	108.00/–/50–500/298	S5
	SDS-γ-Fe_2O_3[d]	166.70/6.0/1–400/298	S6
	NIPAm-*co*-IA[e]	209.20/–/50–500/298	S7
	AAM-IA-MMT[f] hydrogel nanocomposite	457.40/6.0/500/298	S8
	AAm-AMPSNa[g] hydrogel	492.20/–/500/298	S9
	NRCBD[h]	**46.14/9.0/5–40/303**	**TS^**
SF	AC[i]	1.32/5.0/25/298	S10
	hydrogels prepared with sodium polyacrylate and 6 wt% of CM	9.45/–/10/–	S4
	CO_2 neutralized activated red mud	9.77/8.3/37/302	S11
	native SBP[j]	17.90/10.0/100/293	S12
	AC[i]	19.01/6.0/10/–	S13
	pinapple peels	21.70/6.0/60/302	S14
	Cu-NWs-AC[k]	34.00/5.5/15/–	S15
	NaOH-treated rice husk	37.97/8.0/10/303	S16
	MWCNT[l]	43.42/1.0/25/298	S10
	NiS-NP-AC[m]	46.00–52.00/8.1/5/–	S17
	Au-NP-AC[n]	50.25/7.0/18/–	S18
	CuO-NPs[o]	53.67/12.0/154/303	S19
	PDA@SBP[p]	54.00/10.0/100/293	S12
	HDTMA[q]-modified Spirulina sp.	54.05/2.0/300/–	S20
	ZnO-NR-AC[r]	55.25/6.0/10/–	S13
	MIL-101(Cr)-SO_3H	70.80/6.2/50/–	S21
	Al-Mont-EnPILC[s]	76.13/10.0/100/295	S22
	$Cd(OH)_2$-NW-AC[t]	76.92/5.0/25/298	S10
	SDS/RM[u]	89.40/4.0/50/308	S23
	PANIPN21[v]	117.60/9.0/30/303	S24
	PANIPN41[w]	127.61/9.0/30/303	S24
	MDMLG[x]	137.53/12.0/105/–	S25
	NRCBD[h]	**303.61/10.0/5–40/303**	**TS^**
Hg(II)	starch-*g*-poly(acrylamide)	7.30/0.5–1.0/–/293	S26
	chitosan derivative adsorbent	9.02/3.0/60/298	S27
	EDA-modified mPMMA microbeads[y]	9.08/5.0/5–700/298	S28
	RGO[z]-MnO_2	9.50/–/1/303	S29
	RGO[z]-Ag	9.53/–/1/303	S29
	APT[aa]	13.20/5.0/3800/303	S30
	Hardwickia binata bark	13.50/6.0/400/298	S31
	natural chitosan spheres	13.50±0.40/6.0/38–375/298	S32
	mesoporous silica-coated magnetic particles	14.00/2.0/10–60/–	S33
	poly(AAm-*co*-AAc)[ab]	15.50/2.5/100/288	S34
	Ti(IV)[ac]	17.20/6.0/20/293–323	S35
	poly(HEMA[ad]/chitosan) composite membranes	18.41±0.54/2.0–6.0/30–400/293	S36
	SMs[ae]	20.00/7.5/100–900/303	S37
	GMA-MMA-DVB[af]	20.06/7.0/15/298	S38
	chemically treated sawdust (*Acacia arabica*)	20.62/6.0/3/–	S39
	multifunctional mesoporous material	21.05/–/1000/–	S40
	CTS–PVA[ag]	24.98/5.5/50/303	S41
	Ca-alginate beads	28.90±0.70/6.0/200/298	S42
	poly(MMA-MAGA)[ah]	29.90/2.0–6.0/100/293	S42
	epichlorohydrin-crosslinked chitosan membranes	30.30/6.0/38–375/298	S44
	glutaraldehyde-crosslinked chitosan spheres	31.10±0.30/6.0/38–375/298	S32
	BTESPT-SMs[ai]	37.00/7.5/100–900/303	S36

phosphoric acid-treated poly(glycidylmethacrylate-*co*-divinyl benzene)	40.00/–/100/300	S45
GGAMSAASP18[aj]	40.95/7.0/5–30/303	S46
GGAMSAASP14[ak]	49.12/7.0/5–30/303	S46
cellulose-lysine-schiff bases	50.60/4.4/100/303	S47
TCPF[al]	52.63/6.0/50/301	S48
4-aminoantipyrine immobilized bentonite	52.90/4.0/1/298	S49
CNTs/Fe_3O_4[am]	65.52/6.5/50/298	S50
dithiocarbamate-anchored polymer/organosmectite composites	71.10/7.0/50/293	S51
graphene-MWCNT[l]	75.80/–/50/298	S52
PANIPN41[w]	78.44/7.0/30/303	S24
Si-DTC[an]	80.24/6.0/200/298	S53
MWCNTs[l]	84.66/6.0/400/298	S54
graphene/c-MWCNT[l]	93.30/–/50/298	S52
PANIPN21[i]	96.78/7.0/30/303	S24
CSTU[ao]	135.00/5.0/100/303	S55
dithizone-anchored poly(vinyl pyridine)	144.40/3.0/1000/–	S56
3-trimethoxysilyl-1-propanethiol immobilized on silica	186.50/6.0/–/298	S57
PAM/ATP[ap]	192.50/7.0/100–900/303	S58
bayberry tannin-immobilized collagen fiber	198.49/7.0/200/303	S59
polypyrrole-rGO[y]	980.00/3.0/50–250/298	S60
PANI-rGO[aq]	1000.00/4.0/10–40/305	S61
pullulan-graft-polyacrylamide semi-IPN hydrogel	1724.47/6.1/100/292	S62
GGTI-*g*-TetraP1[ar]	1759.50/7.0/500–1000/293	S63
GGTI-*g*-TetraP2[as]	1848.03/7.0/500–1000/293	S63
NRCBD	**166.46/7.0/5–40/303**	**TS^**

[a]copolymer of acrylic acid, hydroxyl ethyl methacrylate (HEMA) and sodium carboxy methyl cellulose (CMC), [b]copolymer of sodium acrylate and CMC, [c]copolymer of acrylic acid and CMC, [d]sodium dodecyl sulfate (SDS) modified maghemite nanoparticles, [e]*N*-isopropylacrylamide-*co*-itaconic acid, [f]*co*-polymer of acrylamide and itaconic acid sodium salt in the presence of montmorillonite, [g]acrylamide-2-acrylamide-2-methylpropanesulfonic acid sodium salt hydrogel, [h]natural rubber (NR) and cow buffing dust (CBD) based scalable biocomposite, [i]activated carbon, [j]sea buckthornbranchpowder, [k]copper nanowires loaded on activated carbon, [l]multiwalled carbon nanotube, [m]nickel sulfide nanoparticle-loaded activated carbon, [n]Au loaded on activated carbon, [o]copper oxide nanoparticles, [p]polydopamine coated sea buckthornbranch powder, [q]hexadecyltrimethylammonium bromide, [r]ZnO nanorod-loaded activated carbon, [s]Al-Mont-EnPILC, [t]cadmium hydroxide nanowire loaded on activated carbon, [u]sodium dodecyl sulphate/red mud, [v]pectin-*g*-(TerP21), [w]pectin-*g*-(TerP41), [x]MgO decked multi-layered graphene, [y]ethylene diamine modified magnetic polymethylmethacrylate microbeads, [z]reduced graphene oxide, [aa]attapulgite, [ab]poly(acrylic acid/acrylamide), [ac]Ti(IV) iodovanadate cation exchanger, [ad]hydroxyethylmethacrylate, [ae]silica microspheres, [af]methyl methacrylate-glycidyl methacrylate-divinylbenzene terpolymer beads, [ag]chitosan–poly(vinyl alcohol), [ah]poly(methyl methacrylate–methacryloylamidoglutamic acid), [ai]bis(triethoxysilylpropyl) tetrasulfide silica microspheres, [aj]guar gum-*g*-(acrylamide-*co*-sodium acrylate-*co*-acrylamidosodium propanoate)18, [ak]guar gum-*g*-(acrylamide-*co*-sodium acrylate-*co*-acrylamidosodium propanoate)14, [al]thiocarbohydrazide cross-linked chitosan-poly(vinyl alcohol) framework, [am]carbon nanotube/magnetite nanocomposites, [an]silica-supported dithiocarbamate adsorbent, [ao]cross-linked magnetic chitosan-phenylthiourea, [ap]polyacrylamide/attapulgite, [aq]polyaniline and rGO, [ar]gum ghatti (GGTI)-*g*-[sodium acrylate (SA)-*co*-4-(acrylamido)-4-methyl pentanoate (AMP)-*co*-3-(*N*-(4-(4-methyl pentanoate)) acrylamido) propanoate (NMPAP)-*co*-*N*-isopropylacrylamide (NIPA)]1, [as]gum ghatti (GGTI)-*g*-[sodium acrylate (SA)-*co*-4-(acrylamido)-4-methyl pentanoate (AMP)-*co*-3-(*N*-(4-(4-methyl pentanoate)) acrylamido) propanoate (NMPAP)-*co*-*N*-isopropylacrylamide (NIPA)]2, and ^this study.

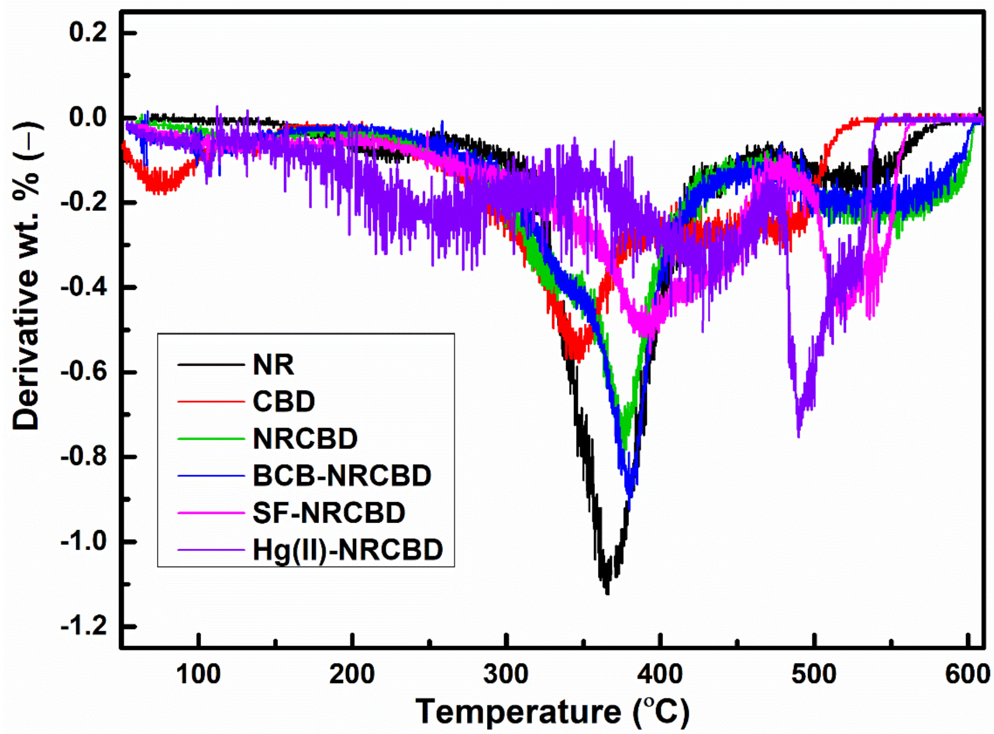

Figure S1. DTG of NR, CBD, NRCBD, BCB-, SF-, and Hg(II)-NRCBD

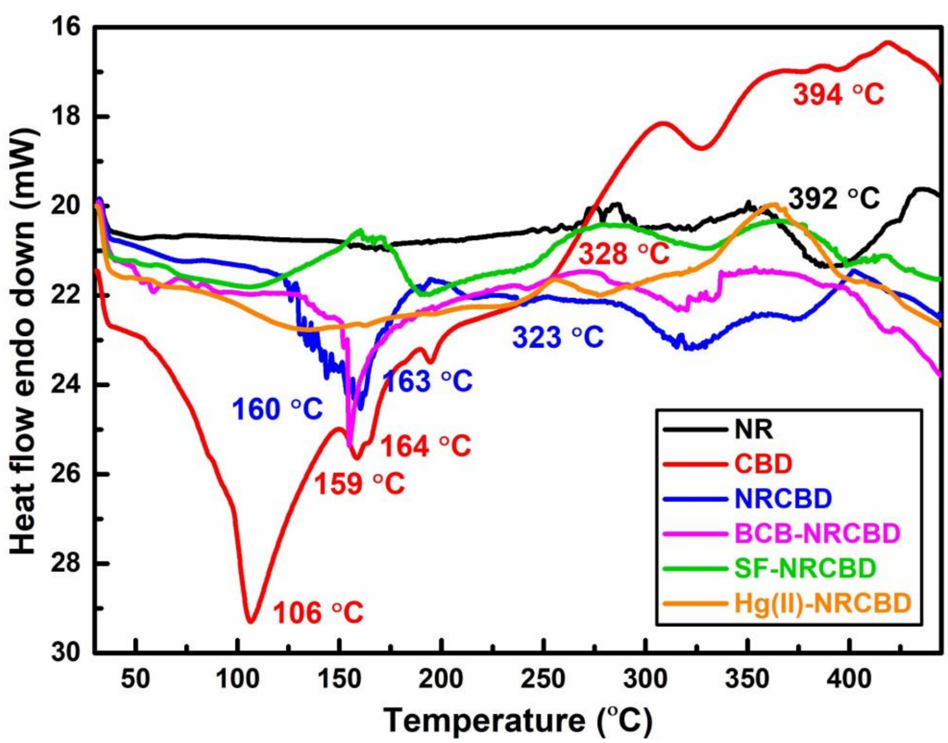

Figure S2. DSC of NR, CBD, NRCBD, BCB-, SF-, and Hg(II)-NRCBD

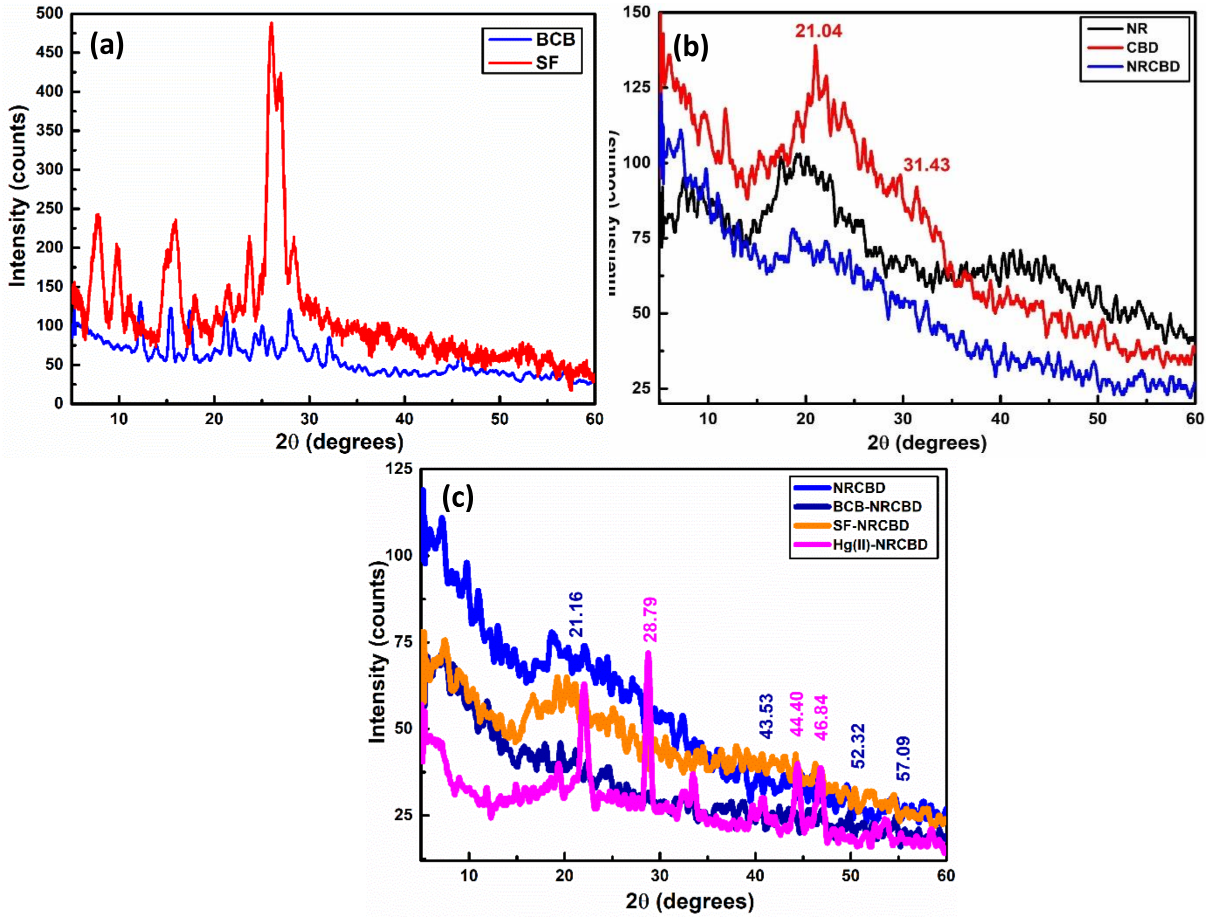

Figure S3. XRD of (a) SF and BCB, (b) NR, CBD, and NRCBD, and (c) NRCBD, BCB-, SF-, and Hg(II)-NRCBD

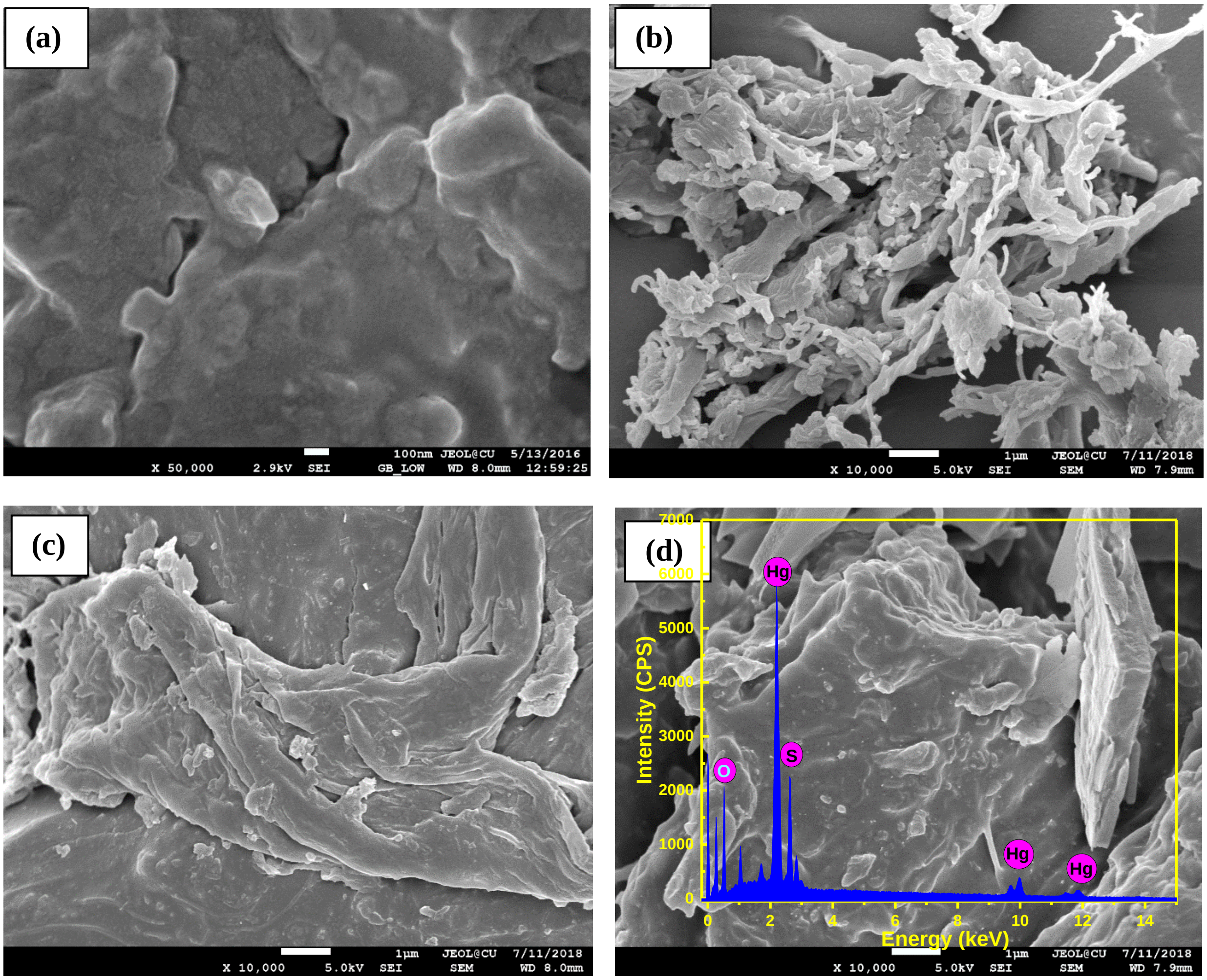

Figure S4. FESEM photomicrographs of (a) NR, (b) CBD, (c) NRCBD, and (d) Hg(II)-NRCBD; (inset of d) EDX of Hg(II)-NRCBD

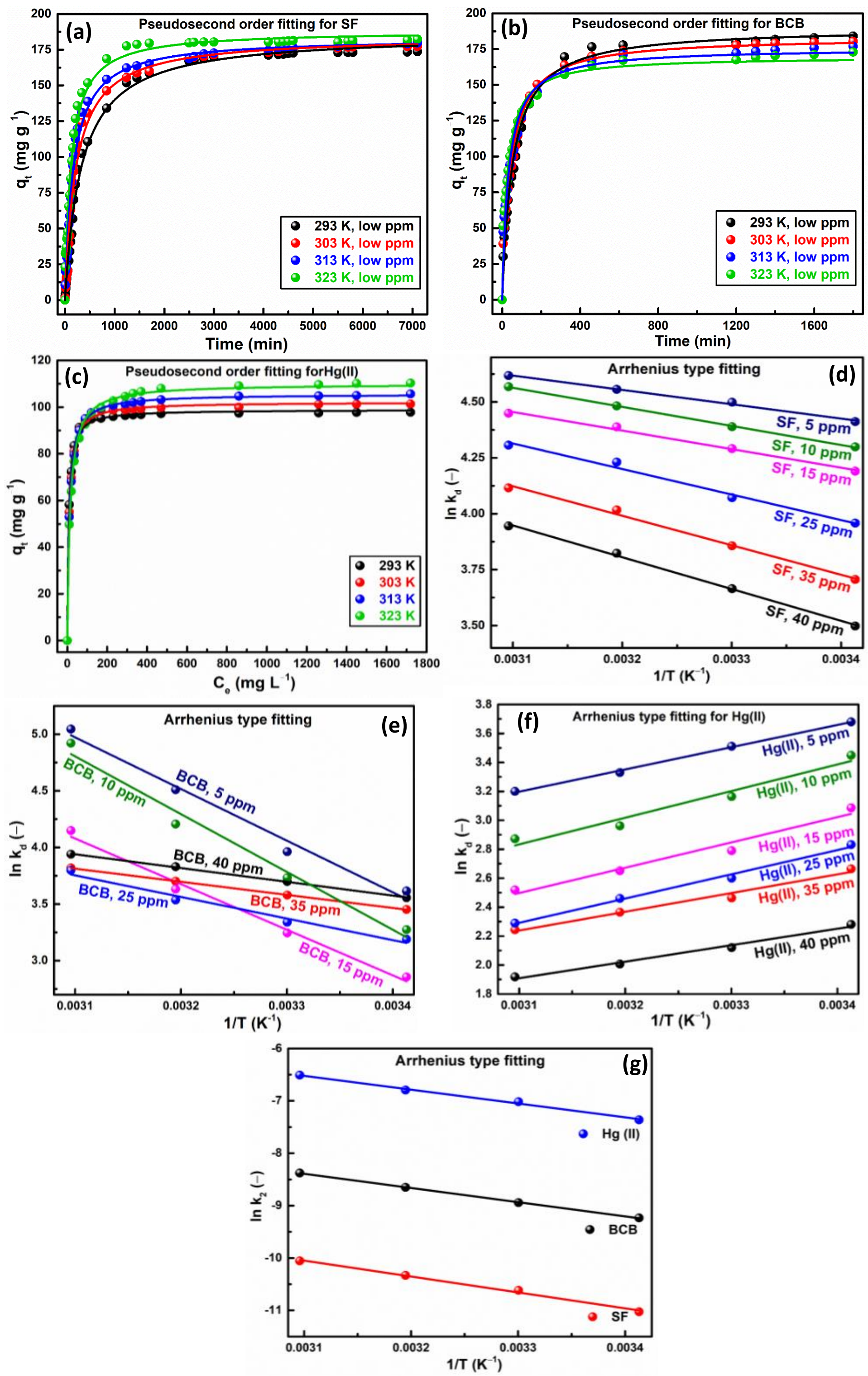

Figure S5. Pseudosecond order fitting of (a) SF-, (b) BCB-, and (c) Hg(II)-NRCBD; Arrhenius type fitting for (d) SF-, (e) BCB-, and (f) Hg(II)-NRCBD and (g) SF-/BCB-, Hg(II)-NRCBD

References

(S1) Steiner, T.; Saenger, W. Geometry of C–H….O Hydrogen Bonds in Carbohydrate Crystal Structures. Analysis of Neutron Diffraction Data. *J. Am. Chem. Soc.* **1992**, *114*, 10146–10154.

(S2) Güçlü, G. Removal of Basic Dyes from Aqueous Solutions by Dimethyl Terephthalate Distillation Residue. *Desalination* **2010**, *259*, 53–58

(S3) Banuİyim, T.; Güçlü, G. Removal of Basic Dyes from Aqueous Solutions using Natural Clay. *Desalination* **2009**, *249*, 1377–1379.

(S4) Mandal, B.; Ray, S. K. Removal of Safranine T and Brilliant Cresyl Blue Dyes from Water by Carboxymethyl Cellulose Incorporated Acrylic Hydrogels: Isotherms, Kinetics and Thermodynamic Study. *J. Taiwan Inst. Chem. E.* **2016**, *60*, 313–327.

(S5) Íyim, T. B.; Acar, I.; Özgümüş, S. Removal of Basic Dyes from Aqueous Solutions with Sulfonated Phenol-Formaldehyde Resin. *J. Appl. Polym. Sci*. **2008**, *109*, 2774–2780.

(S6) Afkhami, A.; Saber-Tehrani, M.; Bagheri, H. Modified Maghemite Nanoparticles as An Efficient Adsorbent for Removing Some Cationic Dyes from Aqueous Solution. *Desalination* **2010**, *263*, 240–248.

(S7) Özkahraman, B.; Acar, I.; Emik, S. Removal of Cationic Dyes from Aqueous Solutions with Poly (*N*-Isopropylacrylamide-*co*-Itaconic Acid) Hydrogels. *Polym. Bull*. **2011**, *66*, 551–570.

(S8) Kaplan, M.; Kasgoz, H. Hydrogel Nanocomposite Sorbents for Removal of Basic Dyes. *Polym. Bull*. **2011**, *67*, 1153–1168.

(S9) Kaşgöz, H.; Durmus, A. Dye Removal by A Novel Hydrogel-Clay Nanocomposite with Enhanced Swelling Properties. *Polym. Adv. Technol*. **2008**, *19*, 838–845.

(S10) Ghaedi, M.; Haghdoust, S.; Nasiri Kokhdan, S.; Mihandoost, A.; Sahraie, R.; Daneshfar, A. Comparison of Activated Carbon, Multiwalled Carbon Nanotubes, and Cadmium Hydroxide Nanowire Loaded on Activated Carbon as Adsorbents for Kinetic and Equilibrium Study of Removal of Safranine O. *Spectrosc. Lett*. **2012**, *45*, 500–510.

(S11) Sahu, M. K.; Sahu, U. K.; Patel, R. K. Adsorption of Safranin-O Dye on CO_2 Neutralized Activated Red Mud Waste: Process Modelling, Analysis and Optimization using Statistical Design. *RSC Adv.* **2015**, *5*, 42294–42304.

(S12) Xu, X.; Bai, B.; Wang, H.; Suo, Y. Enhanced Adsorptive Removal of Safranine T from Aqueous Solutions by Waste Sea Buckthorn Branch Powder Modified with Dopamine: Kinetics, Equilibrium, and Thermodynamics. *J. Phys. Chem. Solids* **2015**, *87*, 23–31.

(S13) Nasiri Azad, F.; Ghaedi, M.; Dashtian, K.; Hajati, S.; Goudarzi, A.; Jamshidi, M. Enhanced Simultaneous Removal of Malachite Green and Safranin O by ZnO Nanorod-Loaded Activated Carbon: Modeling, Optimization and Adsorption Isotherms. *New J. Chem*. **2015**, *39*, 7998–8005.

(S14) Mohammed, M. A.; Ibrahim, A.; Shitu, A. Batch Removal of Hazardous Safranin-O in Wastewater using Pineapple Peels as an Agricultural Waste Based Adsorbent. *Int. J. Environ. Monit. Anal.* **2014**, *2*, 128–133.

(S15) Roosta, M.; Ghaedia, M.; Asfaram, A. Simultaneous Ultrasonic-Assisted Removal of Malachite Green and Safranin O by Copper Nanowires Loaded on Activated Carbon: Central Composite Design Optimization. *RSC Adv.* **2015**, *5*, 57021–57029.

(S16) Chowdhury, S.; Mishra, R.; Kushwaha, P.; Saha, P. Removal of Safranin from Aqueous Solutions by NaOH-Treated Rice Husk: Thermodynamics, Kinetics and Isosteric Heat of Adsorption. *Asia-Pac. J. Chem. Eng.* **2012**, *7*, 236–249.

(S17) Ghaedi, M.; Pakniat, M.; Mahmoudi, Z.; Hajati, S.; Sahraei, R.; Daneshfar, A. Synthesis of Nickel Sulfide Nanoparticles Loaded on Activated Carbon as a Novel Adsorbent for the Competitive Removal of Methylene Blue and Safranin-O. *Spectrochim. Acta A* **2014**, *123*, 402–409.

(S18) Roosta, M.; Ghaedi, M.; Daneshfar, A.; Sahraei, R. Experimental Design Based Response Surface Methodology Optimization of Ultrasonic Assisted Adsorption of Safaranin O by Tin Sulfide Nanoparticle Loaded on Activated Carbon. *Spectrochim. Acta A* **2014**, *122*, 223–231.

(S19) Wahab, R.; Khan, F.; Kaushik, N. K.; Musarrat, J.; Al-Khedhairy, A. A. Photocatalytic TMO-NMs Adsorbent: Temperature-Time Dependent Safranine Degradation, Sorption Study Validated under Optimized Effective Equilibrium Models Parameter with Standardized Statistical Analysis. *Sci. Rep.* **2017**, *7*, 1–15.

(S20) Guler, U. A.; Ersan, M.; Tuncel, E.; Dügenci, F. Mono and Simultaneous Removal of Crystal Violet and Safranin Dyes from Aqueous Solutions by HDTMA-Modified *Spirulina* sp. *Process Saf. Environ.* **2016**, *99*, 194–206.

(S21) Zhao, X.; Wang, K.; Gao, Z.; Gao, H.; Xie, Z.; Du, X.; Huang, H. Reversing the Dyes Adsorption and Separation Performance of Metal-Organic Frameworks *via* Introduction of –SO_3H Groups. *Ind. Eng. Chem. Res.* **2017**, *56*, 4496–4501.

(S22) Tovar-Gómez, R.; Rivera-Ramírez, D. A.; Hernández-Montoya, V.; Bonilla-Petriciolet, A.; Durán-Valle, C. J.; Montes-Morán, M. A. Synergic Adsorption in the Simultaneous Removal of Acid Blue 25 and Heavy Metals from Water using a $Ca(PO_3)_2$-Modified Carbon. *J. Hazard. Mater.* **2012**, *199–200*, 290–300.

(S23) Sahu, M. K.; Patel, R. K. Removal of Safranin-O Dye 1 from Aqueous Solution using Modified Red Mud: Kinetic and Equilibrium Studies. *RSC Adv.* **2015**, *5*, 78491–78501.

(S24) Singha, N. R.; Mahapatra, M.; Karmakar, M.; Mondal, H.; Dutta, A.; Deb, M.; Mitra, M.; Roy, C.; Chattopadhyay, P. K.; Maiti, D. K. In Situ Allocation of a Monomer in Pectin-*g*-Terpolymer Hydrogels and Effect of Comonomer Compositions on Superadsorption of Metal Ions/Dyes. *ACS Omega* **2018**, *3*, 4163–4180.

(S25) Rotte, N. K.; Yerramala, S.; Boniface, J.; Srikanth, V. V. S. S. Equilibrium and Kinetics of Safranin O Dye Adsorption on MgO Decked Multi-Layered Graphene. *Chem. Eng. J.* **2014**, *258*, 412–419.

(S26) Khalil, M. I.; Farag, S. Utilization of Some Starch Derivatives in Heavy Metal Ions Removal. *J. Appl. Polym. Sci.* **1998**, *69*, 45–50.

(S27) Tang, X.; Niu, D.; Bi, C.; Shen, B. Hg^{2+} Adsorption from a Low-Concentration Aqueous Solution on Chitosan Beads Modified by Combining Polyamination with Hg^{2+}-Imprinted Technologies. *Ind. Eng. Chem. Res.* **2013**, *52*, 13120–13127.

(S28) Denizli, A.; Ozkan, G.; Arica, M. Y. Preparation and Characterization of Magnetic Polymethylmethacrylate Microbeads Carrying Ethylene Diamine for Removal of Cu(II), Cd(II), Pb(II), and Hg(II) from Aqueous Solutions. *J. App. Polym. Sci.* **2000**, *78*, 81–89.

(S29) Sreeprasad, T. S.; Maliyekkal, S. M.; Lisha, K. P.; Pradeep, T. Reduced Graphene Oxide-Metal/Metal Oxide Composites: Facile Synthesis and Application in Water Purification. *J. Hazard. Mater.* **2011**, *186*, 921–931.

(S30) Wang, X.; Wang, A. Adsorption Characteristics of Chitosan-*g*-Poly(Acrylic Acid)/Attapulgite Hydrogel Composite for Hg(II) Ions from Aqueous Solution. *Separ. Sci. Technol.* **2010**, *45*, 2086–2094.

(S31) Deshkar, A. M.; Bokade, S. S.; Dara, S. S. Modified *Hardwickia Binata* Bark for Adsorption of Mercury (II) from Water. *Water Res.* **1990**, *24*, 1011–1016.

(S32) Vieira, R. S.; Beppu, M. M. Dynamic and Static Adsorption and Desorption of Hg(II) Ions on Chitosan Membranes and Spheres. *Water Res.* **2006**, *40*, 1726–1734.

(S33) Dong, J.; Xu, Z.; Wang, F. Engineering and Characterization of Mesoporous Silica-Coated Magnetic Particles for Mercury Removal from Industrial Effluents. *Appl. Surf. Sci.* **2008**, *254*, 3522–3530.

(S34) Bingöl, D.; Saraydin, D.; Özbay, D. S. Full Factorial Design Approach to Hg(II) Adsorption onto Hydrogels. *Arab. J. Sci. Eng.* **2015**, *40*, 109–116.

(S35) Naushad, M.; ALOthman, Z. A.; Awual, M. R.; Alam, M. M.; Eldesoky, G. E. Adsorption Kinetics, Isotherms, and Thermodynamic Studies for the Adsorption of Pb^{2+} and Hg^{2+} Metal Ions from Aqueous Medium Using Ti(IV) Iodovanadate Cation Exchanger. *Ionics* **2015**, *21*, 2237–2245.

(S36) Genç, Ö.; Soysal, L.; Bayramoglu, G.; Arıca, M. Y.; Bektas, S. Procion Green H-4G Immobilized Poly(Hydroxyethylmethacrylate/Chitosan) Composite Membranes for Heavy Metal Removal. *J. Hazard. Mater.*, **2003**, *97*, 111–125.

(S37) Saman, N.; Johari, K.; Mat, H. Adsorption Characteristics of Sulfur-Functionalized Silica Microspheres with respect to the Removal of Hg(II) from Aqueous Solutions. *Ind. Eng. Chem. Res.* **2014**, *53*, 1225−1233.

(S38) Bicak, N.; Sherrington, D. C.; Sungur, S.; Tan, N. A Glycidyl Methacrylate-Based Resin with Pendant Urea Groups as a High Capacity Mercury Specific Sorbent. *React. Funct. Polym.* **2003**, *54*, 141–147.

(S39) Meena, A. K.; Kadirvelu, K.; Mishra, G. K.; Rajagopal, C.; Nagar, P. N. Adsorptive Removal of Heavy Metals from Aqueous Solution by Treated Sawdust (*Acacia arabica*). *J. Hazard. Mater.* **2008**, *150*, 604–611.

(S40) Wang, C.; Tao, S.; Wei, W.; Meng, C.; Liu, F.; Han, M. Multifunctional Mesoporous Material for Detection, Adsorption and Removal of Hg^{2+} in Aqueous Solution. *J. Mater. Chem.* **2010**, *20*, 4635–4641.

(S41) Wang, X.; Yang, L.; Zhang, J.; Wang, C.; Li, Q. Preparation and Characterization of Chitosan-Poly(Vinyl Alcohol)/Bentonite Nanocomposites for Adsorption of Hg(II) Ions. *Chem. Eng. J.* **2014**, *251*, 404–412.

(S42) Kacar, Y.; Arpa, C.; Tan, S.; Denizli, A.; Genc, O.; Arica, M. Y. Biosorption of Hg(II) and Cd(II) from Aqueous Solutions: Comparison of Biosorptive Capacity of Alginate and Immobilized Live and Heat Inactivated *Phanerochaete chrysosporium*. *Process Biochem.* **2002**, *37*, 601–610.

(S43) Denizli, A.; Sanli, N.; Garipcan, B.; Patir, S.; Alsancak, G. Methacryloylamidoglutamic Acid Incorporated Porous Poly(Methylmethacrylate) Beads for Heavy-Metal Removal. *Ind. Eng. Chem. Res.* **2004**, *43*, 6095–6101.

(S44) Vieira, R. S.; Beppu, M. M. Interaction of Natural and Crosslinked Chitosan Membranes with Hg(II) Ions. *Colloid. Surface. A* **2006**, *279*, 196–207.

(S45) Jyo, A.; Matsufune, S.; Ono, H.; Egawa, H. Preparation of Phosphoric Acid Resins with Large Cation Exchange Capacities from Macroreticular Poly(Glycidyl Methacrylate-*co*-Divinylbenzene) Beads and their Behavior in Uptake of Metal Ions. *J. Appl. Polym. Sci.* **1997**, *63*, 1327–1334.

(S46) Singha, N. R.; Dutta, A.; Mahapatra, M.; Karmakar, M.; Mondal, H.; Chattopadhyay, P. K.; Maiti, D. K. In Situ Allocation of a Monomer in Pectin-*g*-Terpolymer Hydrogels and Effect of Comonomer Compositions on Superadsorption of Metal Ions/Dyes. *ACS Omega* **2018**, *3*, 472–494.

(S47) Kumari, S.; Chauhan, G. S. New Cellulose-Lysine Schiff-Base-Based Sensor-Adsorbent for Mercury Ions. *ACS Appl. Mater. Inter.* **2014**, *6*, 5908–5917.

(S48) Ahmad, M.; Manzoor, K.; Chaudhuri, R. R.; Ikram, S. Thiocarbohydrazide Cross-Linked Oxidized Chitosan and Poly(Vinyl Alcohol): A Green Framework as Efficient Cu(II), Pb(II), and Hg(II) Adsorbent. *J. Chem. Eng. Data* **2017**, *62*, 2044–2055.

(S49) Wang, Q.; Chang, X.; Li, D.; Hu, Z.; Li, R.; He, Q. Adsorption of Chromium(III), Mercury(II) and Lead(II) Ions onto 4-Aminoantipyrine Immobilized Bentonite. *J. Hazard. Mater*. **2011**, *186*, 1076–1081.

(S50) Zhang, C.; Sui, J.; Li, J.; Tang, Y.; Cai, W. Efficient Removal of Heavy Metal Ions by Thiol-Functionalized Super Paramagnetic Carbon Nanotubes. *Chem. Eng. J.* **2012**, *210*, 45–52.

(S51) Say, R.; Birlik, E.; Denizli, A.; Ersöz, A. Removal of Heavy Metal Ions by Dithiocarbamate-Anchored Polymer/Organosmectite Composites. *Appl. Clay Sci.* **2006**, *31*, 298–305.

(S52) Sui, Z.; Meng, Q.; Zhang, X.; Ma, R.; Cao, B. Green Synthesis of Carbon Nanotube–Graphene Hybrid Aerogels and their Use as Versatile Agents for Water Purification. *J. Mater. Chem.* **2012**, *22*, 8767–8771.

(S53) Bai, L.; Hu, H. P.; Fu, W.; Wan, J.; Cheng, X.; Zhuge, L.; Xiong, L.; Chen, Q. Synthesis of a Novel Silica-Supported Dithiocarbamate Adsorbent and its Properties for the Removal of Heavy Metal Ions. *J. Hazard. Mater.* **2011**, *195*, 261–275.

(S54) Hadavifar, M.; Bahramifar, N.; Younesi, H.; Li, Q. Adsorption of Mercury Ions from Synthetic and Real Wastewater Aqueous Solution by Functionalized Multi-Walled Carbon Nanotube with Both Amino and Thiolated Groups. *Chem. Eng. J.* **2014**, *237*, 217–228.

(S55) Monier, M.; Abdel-Latif, D. A. Preparation of Cross-Linked Magnetic Chitosan-Phenylthiourea Resin for Adsorption of Hg(II), Cd(II) and Zn(II) Ions from Aqueous Solutions. *J. Hazard. Mater.* **2012**, *209–210*, 240–249.

(S56) Shah, R.; Devi, S. Preconcentration of Mercury(II) on Dithizone Anchored Poly(Vinyl Pyridine) Support. *React. Funct. Polym.* **1996**, *31*, l–9.

(S57) Cestari, A. R.; Airoldi, C. Chemisorption on Thiol-Silicas: Divalent Cations as a Function of pH and Primary Amines on Thiol-Mercury Adsorbed. *J. Colloid Interface Sci.* **1997**, *195*, 338–342.

(S58) Zhao, Y.; Chen, Y.; Li, M.; Zhou, S.; Xue, A.; Xing, W. Adsorption of Hg^{2+} from Aqueous Solution onto Polyacrylamide/Attapulgite. *J. Hazard. Mater.* **2009**, *171*, 640–646.

(S59) Huang, X.; Liao, X.; Shi, B. Hg(II) Removal from Aqueous Solution by Bayberry Tannin-Immobilized Collagen Fiber. *J. Hazard. Mater.* **2009**, *170*, 1141–1148.

(S60) Chandra, V.; Kim, K. S. Highly Selective Adsorption of Hg^{2+} by a Polypyrrole-Reduced Graphene Oxide Composite. *Chem. Commun.* **2011**, *47*, 3942–3944.

(S61) Li, R.; Liu, L.; Yang, F. Preparation of Polyaniline/Reduced Graphene Oxide Nanocomposite and its Application in Adsorption of Aqueous Hg(II). *Chem. Eng. J.* **2013**, *229*, 460–468.

(S62) Saber-Samandari, S.; Gazi, M. Pullulan Based Porous Semi-IPN Hydrogel: Synthesis, Characterization and its Application in the Removal of Mercury from Aqueous Solution. *J. Taiwan. Inst. Chem. Eng.* **2015**, *51*, 143–151.

(S63) Mondal, H.; Karmakar, M.; Dutta, A.; Mahapatra, M.; Deb, M.; Mitra, M.; Roy, J. S. D.; Roy, C.; Chattopadhyay, P. K.; Singha, N. R. Tetrapolymer Network Hydrogels *via* Gum Ghatti-Grafted and N−H/C−H-Activated Allocation of Monomers for Composition-Dependent Superadsorption of Metal Ions. *ACS Omega* **2018**, *3*, 10692−10708.